



Undergraduate Honors Theses

2021-06-18

Validity of intrinsic foot muscle size measured by ultrasound and MRI

Dallin Swanson

Follow this and additional works at: https://scholarsarchive.byu.edu/studentpub_uht

BYU ScholarsArchive Citation

Swanson, Dallin, "Validity of intrinsic foot muscle size measured by ultrasound and MRI" (2021).
Undergraduate Honors Theses. 194.
https://scholarsarchive.byu.edu/studentpub_uht/194

This Honors Thesis is brought to you for free and open access by BYU ScholarsArchive. It has been accepted for inclusion in Undergraduate Honors Theses by an authorized administrator of BYU ScholarsArchive. For more information, please contact scholarsarchive@byu.edu, ellen_amatangelo@byu.edu.

Honors Thesis

VALIDITY OF INTRINSIC FOOT MUSCLE SIZE
MEASURED BY MRI AND ULTRASOUND

By
Dallin C. Swanson

Submitted to Brigham Young University in partial fulfillment
of graduation requirements for University Honors

Exercise Sciences Department
Brigham Young University
April 2023

Advisor: A. Wayne Johnson

Honors Coordinator: James D. George

ABSTRACT

VALIDITY OF INTRINSIC FOOT MUSCLE SIZE MEASURED BY MRI AND ULTRASOUND

Dallin C. Swanson

Exercise Sciences Department

Bachelor of Science

Purpose

Intrinsic foot muscles maintain foot structural integrity and contribute to functional movement, posture and balance. Thus, assessing intrinsic foot muscle size and strength are important. Magnetic resonance imaging (MRI) has been shown to accurately image the individual muscles but is costly and time consuming. Ultrasound (US) imaging may provide an alternative that is less costly and more readily available. The purpose of this study was to investigate the validity and reproducibility of US imaging in measuring intrinsic foot muscle size in comparison to MRI.

Methods

US and MRI were employed to measure the intrinsic foot muscle size involving 35 participants (females = 13; males = 22). The scanned intrinsic foot muscles included the flexor hallucis brevis (FHB), abductor hallucis (ABDH), flexor digitorum brevis (FDB), quadratus plantae (QP) and abductor digiti minimi (ADM). Pearson product correlation (r), intraclass correlation coefficients (ICC), standard error of the measurement (SEm) and minimal detectable difference (MDD) were calculated.

Results

High correlations were detected between the US and MRI cross-sectional area (CSA) measurements ($r = 0.971$ to 0.995). Test reliability was excellent for both MRI and US (ICC = 0.994 to 0.999). Sem values for US ranged from 0.026 to 0.044 cm², while the SE_m for MRI ranged from 0.018 to 0.023 cm². MDD values for US ranged from 0.073 to 0.122 cm², while MRI ranged from 0.045 to 0.064 cm².

Conclusion

US appears to be a valid and reliable alternative to MRI when measuring intrinsic foot muscle CSA. While US is less costly and more readily available, the MRI results were shown to be slightly more precise.

ACKNOWLEDGEMENTS

I would like to thank Josh Sponbeck, Derek Swanson, Connor Stevens and Steven Allen for their help throughout the study. I would like to thank Wayne Johnson and Ulrike Mitchell for their guidance and support in creation of the study, data collection and writing of the manuscript. I would like to thank Jim George for overseeing the study and his help moving the study forward.

TABLE OF CONTENTS

TITLE	i
ABSTRACT.....	iii
ACKNOWLEDGEMENTS.....	v
TABLE OF CONTENTS.....	vii
LIST OF FIGURES	viii
LIST OF TABLES	ix
Background.....	1
Methods.....	3
Imaging Preparation.....	3
MRI Scans.....	4
US Imaging	5
Data Processing.....	6
Statistical Analysis.....	Error! Bookmark not defined.
Results.....	7
Discussion.....	7
Limitations	9
Conclusion	10
References.....	11

LIST OF FIGURES

Figure 1. MRI fish oil capsule placement.	14
Figure 2. Location of fish oil capsules in MRI scan.	15
Figure 3. Location of US transducer probe placement.	16
Figure 4. Intrinsic foot muscle images measured by MRI and US.	17
Figure 5. Correlational graphs and Bland-Altman plots – 1 (n=35).	18
Figure 6. Correlational graphs and Bland-Altman plots – 2 (n=35).	19

LIST OF TABLES

Table 1. Mean muscle CSA and correlational coefficient values for US and MRI.....	20
Table 2. Mean ICC and SEM values for US and MRI.....	21
Table 3. Absolute and relative MDD values for US and MRI.....	22

BACKGROUND

Healthy intrinsic foot muscles maintain the structural integrity of the foot (1), are active during functional movement (2), support proper postural alignment (3) and balance control (4). Poor intrinsic foot muscle strength is associated with excessive pronation (5) and pes planus (6). Both excessive pronation and pes planus are associated with several common musculoskeletal overuse injuries and conditions including fatigue, increased navicular drop (7), osteoarthritis (8) and running-related injuries (9). Intrinsic foot muscle atrophy is also related to adverse medical conditions such as Charcot-Marie-Tooth disease (motor and sensory neuropathy), claw toe and hammer toe deformities (10), diabetic neuropathy (11), hallux valgus, pes planus (12), and plantar fasciitis (13). Thus, the ability to accurately and efficiently measure the intrinsic foot muscle size and strength is important in a clinical setting.

Unfortunately, it is inherently challenging to measure the size and strength of the intrinsic foot muscles due to their small size and depth within the foot's tissue structure (12). In addition, these muscles share similar functions, such as maintaining the medial longitudinal arch (14), which makes identifying the specific functional contribution of each intrinsic muscle difficult (10).

Currently, measuring intrinsic foot muscle strength is done using both direct and indirect methods (15). Direct methods are traditional strength diagnostic tests such as paper grip test, plantar pressure, and handheld dynamometry (10, 16). Direct methods measure the combined strength of all intrinsic foot muscles working at the same time but are unable to measure the strength of one specific muscle.

Indirect techniques commonly use the muscle's cross-sectional area (CSA) to estimate intrinsic foot muscle strength (10). Because a muscle's CSA and force production are highly correlated (15, 17), this relationship is regularly used to predict muscle strength (17-19). Indirect techniques can also isolate single muscles (20) and assess muscle size changes during disease states (21) and across exercise training programs (22).

Magnetic resonance imaging (MRI) and ultrasound (US) imaging are both used to indirectly measure intrinsic foot muscle size and estimate muscle strength (23-26). MRI is considered the criterion standard due to its high resolution and multi-planar view (10). MRI is also effective at clearly displaying muscle anatomy by using tissue contrast (27, 28). Although MRI has the great advantage of being able to accurately image individual muscles, it has the disadvantage of being costly and time consuming. In addition, MRI is unable to perform real-time muscle contraction analysis. On the other hand, US imaging measurements may provide a viable alternative that is less costly and more readily available.

Previous research confirms US yields valid CSA measurements as compared to MRI when measuring larger muscles, such as the trapezius (29) tibialis anterior (30) and rectus femoris (31). To date, however, no study has determined the accuracy and validity of US measurements involving the relatively small intrinsic foot muscles.

Consequently, this study's main purpose was to determine whether US can accurately measure the CSA of five intrinsic foot muscles as compared to MRI. A secondary purpose was to compare the reliability of the US and MRI measurements. Our

research hypothesis was that the US method can accurately quantify the CSA of five different intrinsic foot muscles and correlate highly with the MRI method.

METHODS

Thirty-seven participants were recruited for this study, and 35 participants completed all study requirements (female: $n = 13$; mean age \pm SD = 25.4 ± 6.8 years; mean height \pm SD = 180.7 ± 7.0 cm, body mass \pm SD = 82.3 ± 8.9 kg; male: $n = 22$, mean age \pm SD = 23.2 ± 4.6 years, mean height \pm SD = 168.2 ± 5.3 cm, mean body mass \pm SD = 68.7 ± 11.2 kg). Participants were required to be 18 years or older and free from any lower extremity injury within the previous one month or any leg/foot surgery within the previous year. In addition, participants who could not safely receive the MRI scan due to the presence of ferrous-magnetic metal objects within the body, fresh tattoos, a pacemaker, or an implantable cardioverter defibrillator were excluded. Two participants were dropped from the study because of these exclusion criteria.

Each participant read and signed an informed consent form approved by the University's Institutional Review Board (study protocol, IRB2019-375). Each participant completed a safety screen before any MRI testing. Each participant attended one MRI session and one US session. The testing session order was randomized, with each session completed within an hour of one another.

Imaging Preparation

Muscle imaging included scanning the flexor hallucis brevis (FHB), abductor hallucis (ABDH), flexor digitorum brevis (FDB), quadratus plantae (QP), and abductor digiti minimi (ADM). To identify the FHB location, a reference mark was made proximal to the head of the first metatarsal, at 10% of the truncated foot length (32). To image the

other muscles, four reference marks were made perpendicular to the longitudinal axis of the foot's medial, lateral, dorsal, and plantar surface. The medial reference mark was positioned on the navicular tuberosity for both the MRI and US imaging. The other three reference marks were made in the coronal plane in relation to this medial mark. Each 2-mm mark was made on the skin using a Sharpie marker.

MRI Scans

A 3 Tesla magnet (TIM-Trio 3.0T MRI, Siemens, Erlangen, Germany) was employed using a 3-dimensional spoiled gradient echo sequence prescribed with the through-plane direction perpendicular to the long axis of the entire foot. Scan parameters were: TE/TR = 10.8/4.9 ms; matrix size: 416x300x288 pixels; resolution: 0.4x0.4x1 mm; Field of view: 150x108x288 mm; flip angle: 15 degrees; acceleration factor: 2; bandwidth: 130 Hz/pixel; total acquisition time: 4:42. Because each MRI scan was 3-dimensional and contiguous, the data could be reformatted along any direction.

Participants completed an MRI safety screening before entering the magnet room. Before testing, fish oil capsules (Member's Mark, Sam's West Inc., Bentonville, Arkansas) were attached to the participant's skin via double sided Velcro over each reference mark. The capsules were positioned with the long axis parallel to the coronal plane ([Figure 1](#)) and were visible on the MRI images. Each capsule served as a fiducial marker so each MRI scan could be taken at the correct location. The right foot was scanned first. To do so, it was placed in an 8-channel foot/ankle coil (ScanMed, Omaha, NE, USA). The left leg was scanned second. Light sandbags and wedges were employed to minimize foot movement during imaging.

The MRI data were captured as a large-block and formatted to appear as multiple frames. The image that best intersected the reference fish oil capsules was selected for data analysis ([Figure 2](#)). Using the best image reduced placement error to ± 0.5 mm based on the fish oil capsule's diameter and the scan's slice thickness.

US Imaging

Participants were seated in a comfortable back-supported position on a treatment table. During imaging, the participant's hip joint was externally rotated slightly to allow access to the foot's plantar surface. A bolster was placed underneath the participant's knee, with the ankle set at approximately zero degrees dorsiflexion throughout imaging.

Each US muscle image was collected using a ML6-15-D matrix linear transducer probe (LOGIQ S8; GE Healthcare, Chicago, IL), from the transverse/short axis view. Scanning frequencies ranged from 8 to 12 MHz to optimize image clarity. Scanning depth, frequency, focal position, and time-gain-compensation were also adjusted, as needed, to enhance the image quality.

For each US measurement, the transducer probe was placed transversely on the medial-plantar side of the foot over each corresponding mark ([Figure 3](#)). For the FHB, the muscle body was first found by locating the flexor hallucis longus tendon, sesamoid bones and first metatarsal head. The probe was then moved proximally over the FHB reference mark. The ABDH muscle was imaged at the medial midfoot reference mark using the navicular tuberosity. For the FDB, and QP the transducer probe was positioned on the foot's plantar midfoot surface and aligned with the reference marks. The ADM muscle was imaged using the same short axis plane as the ABDH, FDB and QP with the transducer probe positioned at the lateral-plantar midfoot reference mark.

During imaging, participants were asked to contract specific muscles using toe flexion and toe spreading movements. Cine loops recorded the isolated contractions to help identify the muscle's fascial borders and highlight any conformational muscle shape changes (33). Each muscle was imaged in a relaxed state, in a contracted state, and then again in a relaxed state. Two separate recordings of the relax-contract-relax cycle were captured for each muscle. The transducer probe was removed from the foot between recordings.

Data Processing

All MRI scans were loaded into Osirix (Pixmeo, Geneva, Switzerland) to determine the muscle's CSA. Two CSA measurements were taken from adjacent slices at the reference marks, and averaged. Measurements were repeated twice for each specific muscle.

Ultrasound CSA measurements were obtained from a single frame chosen from each cine loop while the muscle was at rest. Images of the muscle's fascial border were captured and analyzed using software on the LOGIQ S8 machine via previously established methods (33, 34). Muscles were imaged on the inside of the muscle fascia border.

Statistical Analysis

Pearson product moment correlations were employed to determine whether the US system generated valid mean CSA results as compared with the MRI system. Intraclass-correlation coefficients ($ICC_{3,1}$) were calculated to establish reliability using CSA measurements from each MRI and US image. To assess image segmentation repeatability, we chose the ICC model with fixed raters and random subjects. To identify

testing error inherent to each imaging modality, we calculated the standard error of the measurement (SEm), a 95% confidence interval, and the minimum detectable difference (MDD) for both MRI and US using the following equations:

$$\text{SEm} = \text{SD} (\text{Sq rt } 1 - r_{\text{ICC}})$$

$$95\% \text{ CI SEm} = \text{muscle mean} \pm (1.96 * \text{SEm})$$

$$\text{MDD} = \text{SEm} * 1.96 * \sqrt{2}$$

Bland-Altman plots were also generated to graphically highlight CSA difference and mean CSA between the MRI and US data, and to visualize any potential systematic error pattern or trends. The x-axis (mean CSA) on the Bland-Altman plots represents the average CSA from the MRI and US data (mean CSA = [MRI CSA + US CSA] ÷ 2) for each participant (n = 35). The y-axis (CSA difference) on the Bland-Altman plots represent the absolute difference between the CSA values (CSA difference = MRI CAS - US CSA) for each participant. Statistical analyses were performed using SPSS version 27.0 statistical software (IBM Corporation, Armonk, NY). An alpha of .05 was employed to determine statistical significance.

RESULTS

High correlations ($r = .971$ to $r = .995$) were computed between the US and MRI mean CSA data, while the Bland-Altman plots indicate no systematic error pattern ([Table 1](#)) and [Figures 5](#) and [6](#). Mean muscle CSA, ICC, and SEm values are outlined in [Table 2](#). The mean muscle CSA values for US range from 2.48 to 1.28 cm², while the MRI values range from 2.53 to 1.28 cm². The SEm values for US range from 0.026 to 0.044 cm², while the MRI values range from 0.018 to 0.023 cm². The ICC values for US range from .991 to .997, while the MRI values range from .997 to .999. The absolute and relative

MDD specific values are summarized in [Table 3](#), with US values ranging from 0.073 to 0.122 cm² and 6.02 to 3.89%, respectively; and MRI values ranging from 0.045 to 0.064 cm² and 2.36 to 4.19%, respectively.

DISCUSSION

The results of this study support our hypotheses. Our findings indicate the US method can reliably quantify the intrinsic foot muscle CSA and also correlates well with the MRI method. Our ICC data (0.991 to 0.999) are slightly higher than in other studies (0.89 to 0.99) that employed US to measure intrinsic foot muscle CSA (24, 25). The most likely reasons for our slightly higher reliability results are our use of cine loops (33) and the fact that we averaged of two separate US measurements (35).

Our CSA correlational results between MRI and US ($r = .971$ to $.995$) are also similar to other studies. For example, Kositsky et al. reported r-values between $.882$ and $.996$ when comparing MRI and US measurements involving the hamstring muscle and hamstring tendon. Similarly, Ahtiainen et al. (36) and Van et al. (37) reported r-values ranging from $.91$ to $.98$ when comparing MRI and US measurements involving the quadriceps and core trunk muscles, respectively. Our Bland-Altman plots further support the high agreement and low error rates between MRI and US.

Our MDD results suggest that the MRI and US protocols can detect a muscle CSA change of about 0.05 cm² and 0.09 cm², respectively ([Table 2](#)). Similarly, Del-Baño Aledo (38) found an average MDD of 0.03 to 0.07 cm² when evaluating the Achilles tendon, patellar tendon and elbow common extensor tendon with US. In terms of relative MDD values, the MRI is able to detect a muscle size change of 2.0% to 4.4%, while US can detect a muscle size change of 3.5% to 6.6% ([Table 3](#)). These values are similar to

those reported in two previous MRI studies evaluating the quadriceps femoris CSA (2.2% to 4.4%) and calf muscle CSA (39, 40). Small MDD values are important when monitoring patients before, during, or after an exercise program to know that changes in muscle size are most likely due to actual muscle size changes and not because of spurious measurement error.

Importantly, our results demonstrate that US is a valid modality to determine intrinsic foot muscle CSA. These results are both statistically significant and clinically significant. Statistically our results exceed a confidence level of 99%, or an approximate 1% probability that our findings are due to random chance (Table 1). Clinically our results are significant since they indicate US measurements are relatively accurate and closely match the corresponding MRI data. Consequently, clinicians can choose to use US if they wish, with the confidence that the intrinsic foot muscle CSA measurements will be comparable to MRI. This is especially meaningful since the US equipment and methodology is 1) widely available, 2) relatively inexpensive, 3) time-efficient, 4) safe, 5) able to show individual real-time muscle activation through cine loops(33), and 6) able to provide immediate muscle CSA results and post-measurement exercise training recommendations (41). Nevertheless, our findings support the MRI protocol as the criterion standard, since it provides slightly more consistent results than US, with lower SEM and MDD values when measuring intrinsic foot muscle CSA.

LIMITATIONS

There are two potential limitations of this study. First, we only recruited young-adult and middle-age participants which suggests that our results cannot be generalized to other age groups. Second, we did not measure all the intrinsic foot muscles.

Consequently, our MRI and US accuracy comparisons may be slightly different had we chosen to measure other intrinsic foot muscles.

CONCLUSION

Although US offers many practical advantages, our results confirm MRI as the criterion measure with higher precision and reliability compared to US when measuring intrinsic foot muscle CSA. In comparison to MRI, our results suggest US yields relatively accurate and reliable intrinsic foot muscle CSA measurements, making US a viable alternative to MRI in the clinical setting.

REFERENCES

1. Allen RH, Gross MT. Toe flexors strength and passive extension range of motion of the first metatarsophalangeal joint in individuals with plantar fasciitis. *Journal of Orthopaedic & Sports Physical Therapy*. 2003;33(8):468-78.
2. Fiolkowski P, Brunt D, Bishop M, Woo R, Horodyski M. Intrinsic pedal musculature support of the medial longitudinal arch: an electromyography study. *The Journal of foot and ankle surgery*. 2003;42(6):327-33.
3. Kelly LA, Kuitunen S, Racinais S, Cresswell AG. Recruitment of the plantar intrinsic foot muscles with increasing postural demand. *Clinical biomechanics*. 2012;27(1):46-51.
4. Mulligan EP, Cook PG. Effect of plantar intrinsic muscle training on medial longitudinal arch morphology and dynamic function. *Manual therapy*. 2013;18(5):425-30.
5. Pabón-Carrasco M, Castro-Méndez A, Vilar-Palomo S, Jiménez-Cebrián AM, García-Paya I, Palomo-Toucedo IC. Randomized clinical trial: The effect of exercise of the intrinsic muscle on foot pronation. *International journal of environmental research and public health*. 2020;17(13):4882.
6. Unver B, Erdem EU, Akbas E. Effects of short-foot exercises on foot posture, pain, disability, and plantar pressure in Pes Planus. *Journal of sport rehabilitation*. 2019;29(4):436-40.
7. Headlee DL, Leonard JL, Hart JM, Ingersoll CD, Hertel J. Fatigue of the plantar intrinsic foot muscles increases navicular drop. *Journal of Electromyography and Kinesiology*. 2008;18(3):420-5.
8. Kaufman KR, Brodine SK, Shaffer RA, Johnson CW, Cullison TR. The effect of foot structure and range of motion on musculoskeletal overuse injuries. *The American journal of sports medicine*. 1999;27(5):585-93.
9. Taddei UT, Matias AB, Duarte M, Sacco IC. Foot Core Training to Prevent Running-Related Injuries: A Survival Analysis of a Single-Blind, Randomized Controlled Trial. *The American Journal of Sports Medicine*. 2020;48(14):3610-9.
10. Soysa A, Hiller C, Refshauge K, Burns J. Importance and challenges of measuring intrinsic foot muscle strength. *Journal of foot and ankle research*. 2012;5(1):1-14.
11. Severinsen K, Obel A, Jakobsen J, Andersen H. Atrophy of foot muscles in diabetic patients can be detected with ultrasonography. *Diabetes care*. 2007;30(12):3053-7.
12. Gooding TM, Feger MA, Hart JM, Hertel J. Intrinsic foot muscle activation during specific exercises: a T2 time magnetic resonance imaging study. *Journal of athletic training*. 2016;51(8):644-50.
13. McKeon PO, Hertel J, Bramble D, Davis I. The foot core system: a new paradigm for understanding intrinsic foot muscle function. *British journal of sports medicine*. 2015;49(5):290-.
14. Chang R, Kent-Braun JA, Hamill J. Use of MRI for volume estimation of tibialis posterior and plantar intrinsic foot muscles in healthy and chronic plantar fasciitis limbs. *Clinical Biomechanics*. 2012;27(5):500-5.

15. Kurihara T, Yamauchi J, Otsuka M, Tottori N, Hashimoto T, Isaka T. Maximum toe flexor muscle strength and quantitative analysis of human plantar intrinsic and extrinsic muscles by a magnetic resonance imaging technique. *Journal of foot and ankle research*. 2014;7(1):1-6.
16. Mickle KJ, Chambers S, Steele JR, Munro BJ. A novel and reliable method to measure toe flexor strength. *Clinical biomechanics*. 2008;23(5):683.
17. Mohseny B, Nijhuis TH, Hundepool CA, Janssen WG, Selles RW, Coert JH. Ultrasonographic quantification of intrinsic hand muscle cross-sectional area; reliability and validity for predicting muscle strength. *Archives of physical medicine and rehabilitation*. 2015;96(5):845-53.
18. Arokoski MH, Arokoski JP, Haara M, Kankaanpää M, Vesterinen M, Niemitukia LH, et al. Hip muscle strength and muscle cross sectional area in men with and without hip osteoarthritis. *The Journal of rheumatology*. 2002;29(10):2185-95.
19. Peltonen JE, Taimela S, Erkintalo M, Salminen JJ, Oksanen A, Kujala UM. Back extensor and psoas muscle cross-sectional area, prior physical training, and trunk muscle strength—a longitudinal study in adolescent girls. *European journal of applied physiology and occupational physiology*. 1997;77(1):66-71.
20. Song H, Israel E, Srinivasan S, Herr H. Pressure based MRI-compatible muscle fascicle length and joint angle estimation. *Journal of neuroengineering and rehabilitation*. 2020;17(1):1-11.
21. Henderson AD, Johnson AW, Rasmussen LG, Peine WP, Symons SH, Scoresby KA, et al. Early-stage diabetic neuropathy reduces foot strength and intrinsic but not extrinsic foot muscle size. *Journal of diabetes research*. 2020;2020.
22. Franchi MV, Longo S, Mallinson J, Quinlan JI, Taylor T, Greenhaff PL, et al. Muscle thickness correlates to muscle cross-sectional area in the assessment of strength training-induced hypertrophy. *Scandinavian journal of medicine & science in sports*. 2018;28(3):846-53.
23. Johnson A, Myrer J, Mitchell U, Hunter I, Ridge S. The effects of a transition to minimalist shoe running on intrinsic foot muscle size. *International journal of sports medicine*. 2016;37(02):154-8.
24. Mickle KJ, Nester CJ, Crofts G, Steele JR. Reliability of ultrasound to measure morphology of the toe flexor muscles. *Journal of Foot and Ankle research*. 2013;6(1):12.
25. Crofts G, Angin S, Mickle KJ, Hill S, Nester C. Reliability of ultrasound for measurement of selected foot structures. *Gait & posture*. 2014;39(1):35-9.
26. Ridge ST, Olsen MT, Bruening DA, Jurgensmeier K, Griffin D, Davis IS, et al. Walking in minimalist shoes is effective for strengthening foot muscles. 2018.
27. Verdú-díaz J, Alonso-Pérez J, Nuñez-Peralta C, Tasca G, Vissing J, Straub V, et al. P. 301Myo-Guide: A new artificial intelligence MRI-based tool to aid diagnosis of patients with muscular dystrophies. *Neuromuscular Disorders*. 2019;29:S155.
28. Bembem MG. Use of diagnostic ultrasound for assessing muscle size. *Journal of Strength and Conditioning Research*. 2002;16(1):103-8.
29. O'Sullivan C, Meaney J, Boyle G, Gormley J, Stokes M. The validity of rehabilitative ultrasound imaging for measurement of trapezius muscle thickness. *Manual therapy*. 2009;14(5):572-8.

30. Sponbeck JK, Frandsen CR, Ridge ST, Swanson DA, Swanson DC, Johnson AW. Leg muscle cross-sectional area measured by ultrasound is highly correlated with MRI. *Journal of Foot and Ankle Research*. 2021;14(1):1-7.
31. Scott JM, Martin DS, Ploutz-Snyder R, Caine T, Matz T, Arzeno NM, et al. Reliability and validity of panoramic ultrasound for muscle quantification. *Ultrasound in medicine & biology*. 2012;38(9):1656-61.
32. Butler RJ, Hillstrom H, Song J, Richards CJ, Davis IS. Arch height index measurement system: establishment of reliability and normative values. *Journal of the American Podiatric Medical Association*. 2008;98(2):102-6.
33. Johnson AW, Stoneman P, McClung MS, Van Wagoner N, Corey TE, Bruening DA, et al. Use of cine loops and structural landmarks in ultrasound image processing improves reliability and reduces error in the assessment of foot and leg muscles. *Journal of Ultrasound in Medicine*. 2020;39(6):1107-16.
34. Johnson AW, Bruening DA, Violette VA, Perkins KV, Thompson CL, Ridge ST. Ultrasound Imaging Is Reliable for Tibialis Posterior Size Measurements. *Journal of Ultrasound in Medicine*. 2020;39(12):2305-12.
35. Koppenhaver SL, Parent EC, Teyhen DS, Hebert JJ, Fritz JM. The effect of averaging multiple trials on measurement error during ultrasound imaging of transversus abdominis and lumbar multifidus muscles in individuals with low back pain. *Journal of orthopaedic & sports physical therapy*. 2009;39(8):604-11.
36. Ahtiainen JP, Hoffren M, Hulmi JJ, Pietikäinen M, Mero AA, Avela J, et al. Panoramic ultrasonography is a valid method to measure changes in skeletal muscle cross-sectional area. *European journal of applied physiology*. 2010;108(2):273-9.
37. Van K, Hides JA, Richardson CA. The use of real-time ultrasound imaging for biofeedback of lumbar multifidus muscle contraction in healthy subjects. *Journal of Orthopaedic & Sports Physical Therapy*. 2006;36(12):920-5.
38. del Baño-Aledo ME, Martínez-Payá JJ, Ríos-Díaz J, Mejías-Suárez S, Serrano-Carmona S, de Groot-Ferrando A. Ultrasound measures of tendon thickness: Intra-rater, Inter-rater and Inter-machine reliability. *Muscles, ligaments and tendons journal*. 2017;7(1):192.
39. Commean PK, Tuttle LJ, Hastings MK, Strube MJ, Mueller MJ. Magnetic resonance imaging measurement reproducibility for calf muscle and adipose tissue volume. *Journal of Magnetic Resonance Imaging*. 2011;34(6):1285-94.
40. Barnouin Y, Butler-Browne G, Voit T, Reversat D, Azzabou N, Leroux G, et al. Manual segmentation of individual muscles of the quadriceps femoris using MRI: a reappraisal. *Journal of Magnetic Resonance Imaging*. 2014;40(1):239-47.
41. Hides J, Richardson C, Jull G, Davies S. Ultrasound imaging in rehabilitation. *Australian Journal of Physiotherapy*. 1995;41(3):187-93.



Figure 1. MRI fish oil capsule placement.



Figure 2. Location of fish oil capsules in MRI scan.



Figure 3. Location of US transducer probe placement.

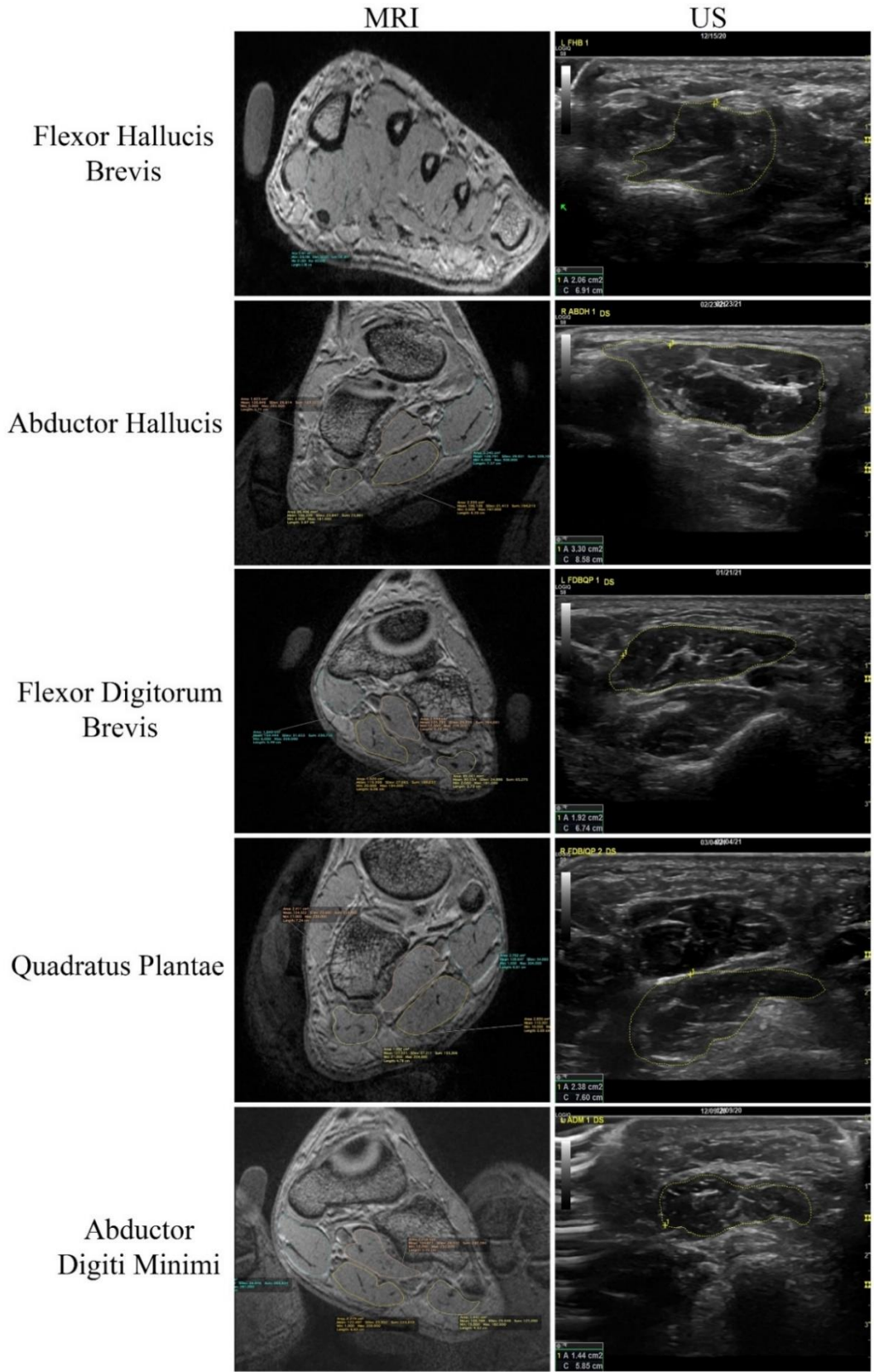


Figure 4. Intrinsic foot muscle images measured by MRI and US.

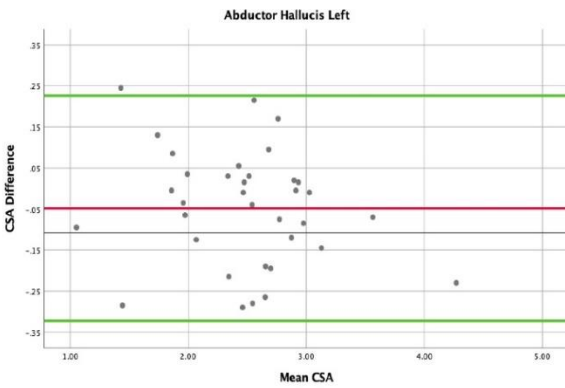
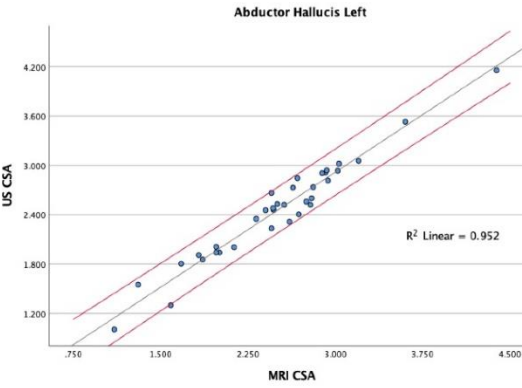
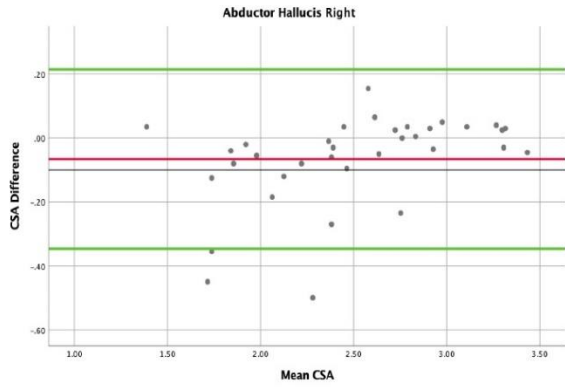
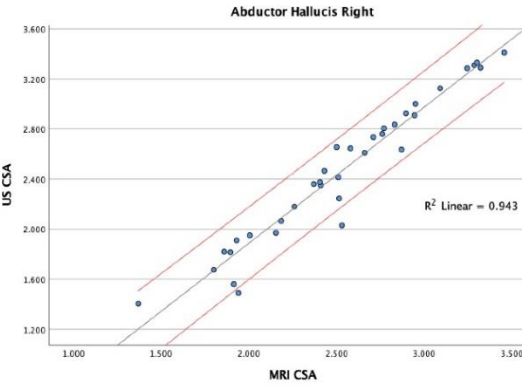
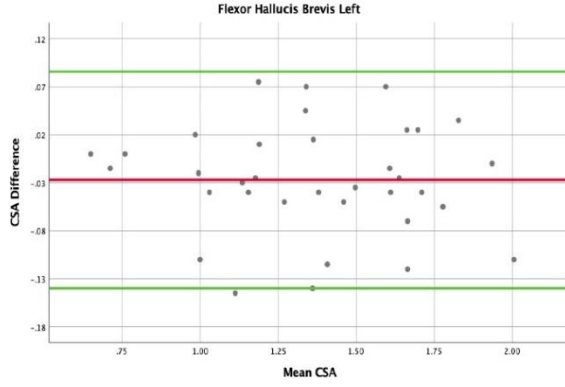
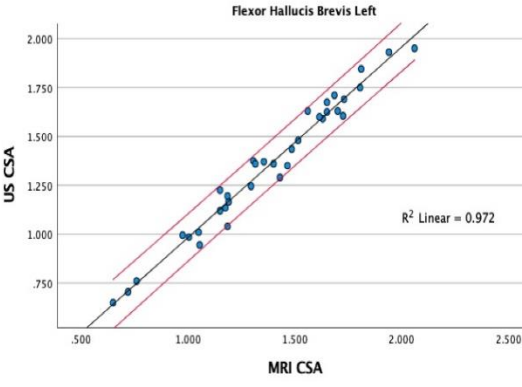
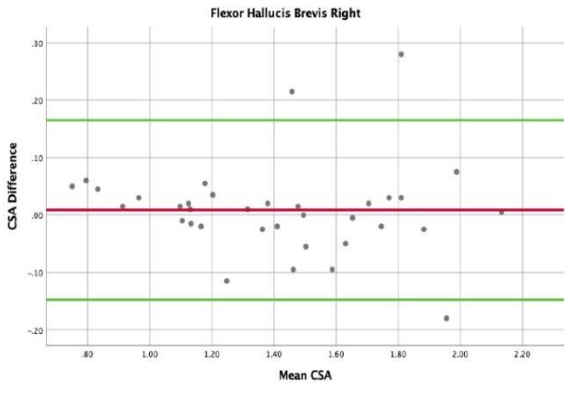
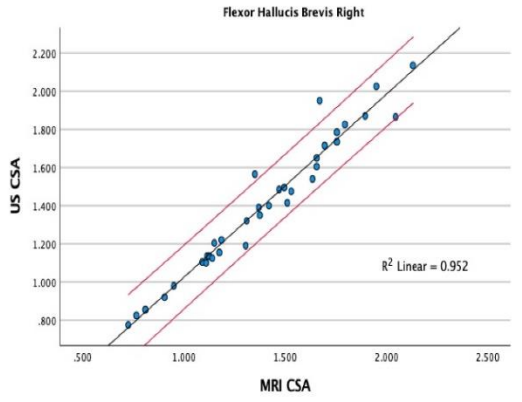


Figure 5. Correlational graphs and Bland-Altman plots – 1 (n=35).

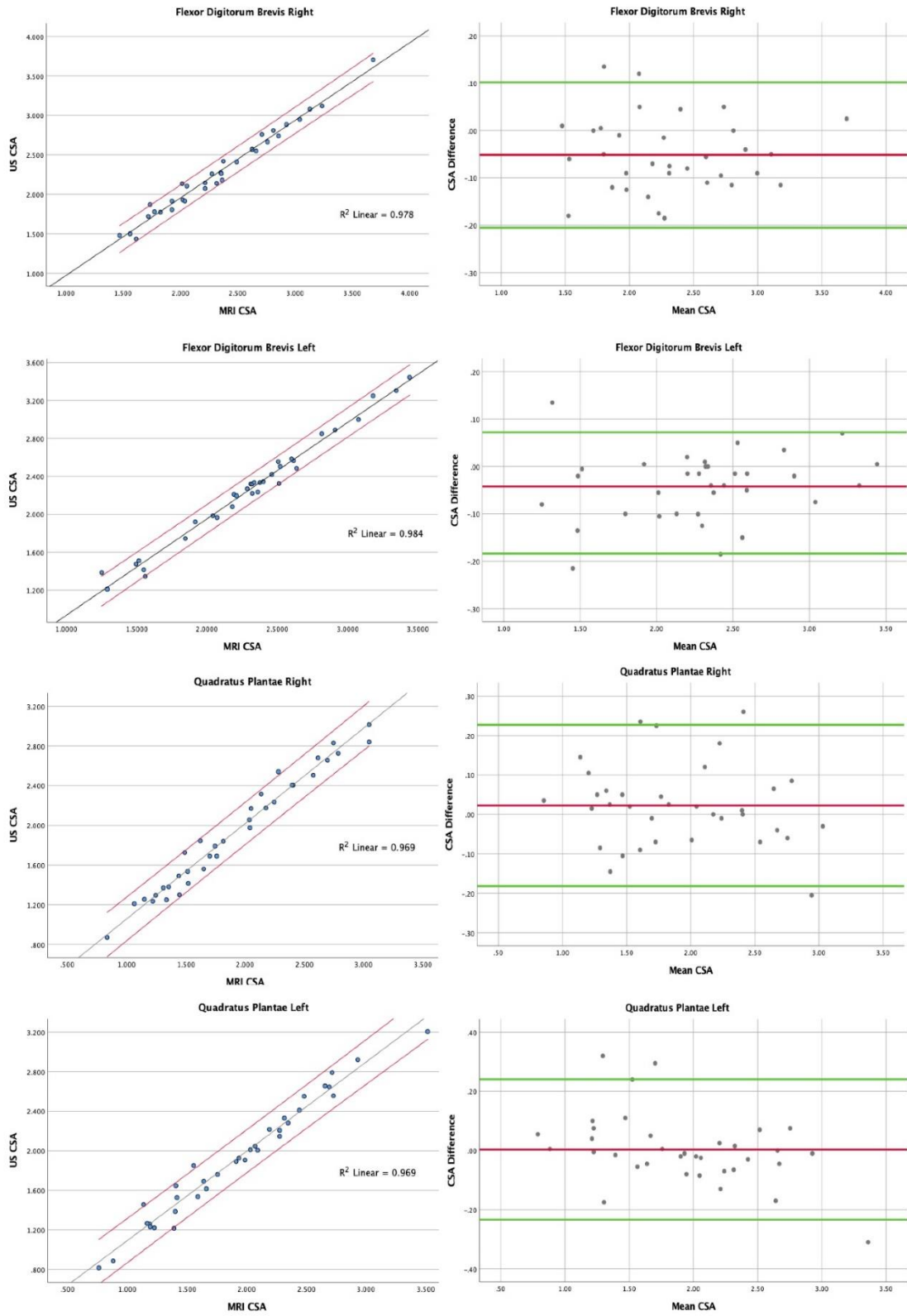


Figure 6. Correlational graphs and Bland-Altman plots – 2 (n=35).

Table 1. Mean muscle CSA and correlational coefficient values for US and MRI.

Muscle	Right foot			Left foot		
	US - CSA	MRI - CSA	r*	US - CSA	MRI - CSA	r*
FHB	1.41 ± 0.36	1.40 ± 0.36	.976	1.36 ± 0.34	1.37 ± 0.35	.986
ABDH	2.48 ± 0.57	2.53 ± 0.51	.971	2.46 ± 0.6	2.51 ± 0.63	.976
FDB	2.29 ± 0.53	2.36 ± 0.52	.989	2.27 ± 0.56	2.32 ± 0.54	.992
QP	1.92 ± 0.58	1.90 ± 0.59	.985	1.92 ± 0.58	1.91 ± 0.64	.985
ADM	1.28 ± 0.37	1.27 ± 0.37	.985	1.29 ± 0.34	1.28 ± 0.33	.995

CSA = cross-sectional area (cm²; mean ± SD), r = Pearson product correlations, FHB = flexor hallucis brevis, ABDH = abductor hallucis, FDB = flexor digitorum brevis, QP = quadratus plantae, ADM = abductor digiti minimi. * All r-values significant at p < .0001.

Table 2. Mean ICC and SEM values for US and MRI.

Right foot				
Muscle	US - ICC _{3,1} (95% CI)	MRI - ICC _{3,1} (95% CI)	US - SEM (95% CI)	MRI - SEM (95% CI)
FHB	.994 (.989, .997)	.998 (.995, .999)	.028 (1.35, 1.46)	.020 (1.37, 1.43)
ABDH	.997 (.994, .998)	.998 (.995, .999)	.031 (2.41, 2.53)	.023 (2.49, 2.58)
FDB	.993 (.985, .996)	.998 (.997, .999)	.044 (2.2, 2.37)	.023 (2.31, 2.4)
QP	.997 (.995, .999)	.999 (.997, .999)	.032 (1.86, 1.98)	.019 (1.86, 1.94)
ADM	.994 (.989, .997)	.997 (.994, .998)	.029 (1.22, 1.33)	.020 (1.23, 1.31)
Left foot				
FHB	.991 (.982, .995)	.997 (.995, .999)	.032 (1.29, 1.42)	.020 (1.34, 1.41)
ABDH	.996 (.991, .998)	.999 (.998, .999)	.038 (2.38, 2.53)	.012 (2.47, 2.54)
FDB	.996 (.993, .998)	.999 (.997, .999)	.035 (2.2, 2.33)	.017 (2.28, 2.35)
QP	.996 (.993, .998)	.999 (.998, 1.00)	.037 (1.84, 1.99)	.020 (1.87, 1.95)
ADM	.994 (.989, .997)	.997 (.993, .998)	.026 (1.24, 1.34)	.018 (1.25, 1.32)

All values reported in cm². ICC = intraclass correlation coefficients, SEM = standard error of the measurement, FHB = flexor hallucis brevis, ABDH = abductor hallucis, FDB = flexor digitorum brevis, QP = quadratus plantae, ADM = abductor digiti minimi.

Table 3. Absolute and relative MDD values for US and MRI.

Muscle	US		MRI	
	Absolute MDD	Relative MDD %	Absolute MDD	Relative MDD %
FHB	.084	6.02	.049	3.54
ABDH	.096	3.89	.060	2.36
FDB	.110	4.82	.056	2.37
QP	.095	4.95	.054	2.83
ADM	.077	5.95	.054	4.19

Average MDD values derived from combined left and right foot data (cm²). Absolute minimum detectable difference (MDD) values calculated using $MDD = SEM * 1.96 * \sqrt{2}$. Relative MDD values calculated using $MDD\% = [MDD / CSA \text{ average}] * 100$.